Separation Science and Technology
Publication details, including instructions for authors and subscription information:
http://www.informaworld.com/smpp/title~content=t713708471

Optimization of the Production of Hydrogen From Syngas Using a 1:7 Mass Ratio of Hematite to Calcium Oxide in a Pressurized Fluidized Bed

Linda S. Denton[a]; Ed Hippo[a]; Tomecz Wiltowski[a]
[a] Department of Mechanical Engineering and Energy Processes, Southern Illinois University, Carbondale, IL, USA

To cite this Article Denton, Linda S. , Hippo, Ed and Wiltowski, Tomecz(2006) 'Optimization of the Production of Hydrogen From Syngas Using a 1:7 Mass Ratio of Hematite to Calcium Oxide in a Pressurized Fluidized Bed', Separation Science and Technology, 41: 4, 665 — 682
To link to this Article: DOI: 10.1080/01496390500527076
URL: http://dx.doi.org/10.1080/01496390500527076

Separation Science and Technology, 41: 665–682, 2006

ISSN 0149-6395 print/1520-5754 online
DOI: 10.1080/01496390500527076

Optimization of the Production of Hydrogen From Syngas Using a 1 : 7 Mass Ratio of Hematite to Calcium Oxide in a Pressurized Fluidized Bed

Linda S. Denton, Ed Hippo, and Tomecz Wiltowski
Department of Mechanical Engineering and Energy Processes, Southern Illinois University, Carbondale, IL, USA

Abstract: A set of response surface experiments were designed to determine the optimum conditions for the production of high-purity hydrogen from wet syngas of composition (44% CO, 23% steam, and 33% hydrogen) using 50 grams of a 1 : 7 mass ratio of Fe_2O_3: CaO loaded into the fluidized bed reactor. Pressure was varied between 50 psi and 515 psi and temperature between 725°C and 800°C. Results indicated:

- High purity hydrogen production is possible at reactor conditions of 725°C & 50 psi, as well as 725°C & 250 psi;
- Optimum high purity hydrogen production (largest mass in 15 minutes with no CO_x) occurred near conditions of 725°C and 250 psi;
- Mass of produced high-purity hydrogen increased most significantly with pressure;
- Methane production increased linearly with pressure due to the catalytic effect of the high nickel content of the reactor walls;
- The chemical reaction rate is predicted to be a controlling factor in the percentage of CO and CO_2 in the outlet at lower pressures.

Keywords: High purity hydrogen, syngas, hematite, calcium oxide, fludidized bed

Received 22 June 2005, Accepted 27 November 2005
Address correspondence to Linda S. Denton, Ph.D., Department of Mechanical Engineering and Energy Processes, Southern Illinois University, Carbondale, IL 62901, USA. E-mail: ldenton@accessus.net

INTRODUCTION

The surge in interest in developing fuel cells for commercial use as a primary electrical production technology has spurred research in methods for production of high purity hydrogen as a fuel source for the fuel cells. Using syngas, with a composition representative of a coal gasifying system, as the feedgas, this study investigates the feasibility and optimization of high purity hydrogen in a high temperature, high pressure fluidized bed using a 1 : 7 mass ratio of Fe_2O_3: CaO as sorbents in a single step operation. The ferric oxide acts as a solid oxygen carrier and calcium oxide as a carbon dioxide absorber. Eventually, the reactor sorbents will be cycled through a regenerator, utilizing an oxygen and steam gas feed.

The production of high-purity hydrogen for fuel cell use holds great promise as a fuel source for the near future. This production can be very cost-effective if low cost sorbents can be used in a one-step process to isolate the hydrogen from natural gas or gasification products. Han and Harrison (1) successfully produced high purity hydrogen in a packed bed reactor combining the Water Gas Shift (WGS) with CO_2 adsorption through the use of CaO. During its reduction to wustite (FeO), hematite shifts the equilibrium ration of CO/CO_x, allowing the more effective use of CaO as a sorbent, and hopefully lessening the expense by extending the sorbent's productivity through several regeneration cycles. A high pressure, high temperature fluidized bed should optimize gas-solid contact and reaction rates and should result in a highly pure hydrogen product gas.

In the high-pressure, high-temperature fluidized bed system, syngas composed of 44% CO, 23% steam, and 33% hydrogen, mole ratios similar to a Vision-21 gasifier, was introduced to the reactor, where a portion of the carbon monoxide combined with the WGS to produce H_2 and CO_2. The remaining CO should theoretically be oxidized by a reaction with ferric oxide, which is reduced to ferrous oxide and then adsorbed by the calcium oxide in a carbonation process. The gas stream exiting the reactor should then consist of high-purity hydrogen in steam.

Thermodynamic properties (2) of the iron and calcium reactions indicate that the reactor process is feasible between the temperatures of 725–900°C. Between these temperatures, the Gibb's Free energy favors the formation of $CaCO_3$ over CaO, and the formation of Fe_3C is suppressed. Based on the theoretical heat of reaction and stoichiometry listed in Table 1, high purity hydrogen generation is feasible. The fact that these compounds are relatively inexpensive and readily available, make them attractive to larger scale studies and industrial applications.

An increase in temperature and pressure is expected to increase the rate of reaction for both the decomposition and oxidation of the iron compounds (3,4). The Boudouard reaction should not be significant if the operating temperature is over 600°C and the decomposition process is halted before elemental iron. An inlet reactor gas composed of hydrogen and carbon monoxide will further increase the rate of reaction, but will contribute to sintering (5,6).

Table 1. Chemical processes and heat of reactions for reactor

Generator reactions	Heat of reaction at 25°C (ΔH_r) kcal/mol
$Fe_2O_3 + CO = 2FeO + CO_2$	+0.31
$CO + H_2O = CO_2 + H_2$	−9.5
$CO_2 + CaO = CaCO_3$	−39.9

Temperature and CO_2 partial pressure should have the greatest effect on the calcium carbonate-calcium oxide reactions in this study (7). Low partial pressure of CO_2 will optimize the calcination process, while a high partial pressure will optimize the recarbonation process. High temperatures increase the rate of reaction, but sintering occurs even at temperatures near 700°C, with enhanced sintering occurring in a carbon dioxide atmosphere (8). Pressures of 15 atmospheres in the cycling process seem to decrease the capacity of CaO, which will be a determining factor in sorbent life (9).

Preliminary thermogravimetric studies of the kinetics of the carbonation of the calcium oxide samples indicated a very fast surface reaction, with the rate controlled by chemical reaction, followed by a slower reaction whose rate is controlled by diffusion through a resistant $CaCO_3$ layer. Only a 33% weight increase was noted over a one-hour period, under a CO_2 atmosphere heated from 50–900°C. Total carbonation requires a 78.5% weight increase. It was theorized that higher pressures could enhance the gaseous diffusion through the product layer. Initial studies of the kinetics, also with a thermogravimetric analyzer, of the reduction of the iron oxide samples indicated a very fast reaction, with reduction to FeO occurring within approximately 10 minutes under a CO atmosphere at 450°C.

The rate of reduction and carbonation, based on time for mass changes in the TGA, indicate a workable mass ratio of 1 : 7 for Fe_2O_3:CaO. This should allow the hematite to reduce near wustite (FeO), while allowing the calcium oxide to totally carbonate.

Addition of inexpensive hematite to the hydrogen production cycle should enhance the process by adding an increase in energy through the exothermic oxidation process and by shifting the CO/CO_2 equilibrium ratio of the WGS.

EXPERIMENTAL APPARATUS

A fluidized bed reactor capable of withstanding temperatures of 820°C and pressures of 35 atmospheres was constructed of Inconel 810 HT. It consisted of a three inch double extra heavy gauge exterior pipe, with a suspended schedule 40 Inconel one inch pipe serving as the actual reactor as shown in Fig. 1. The interior pipe was welded and sealed to a flange, which was sandwiched between two 3″, 900-pound flanges welded to the

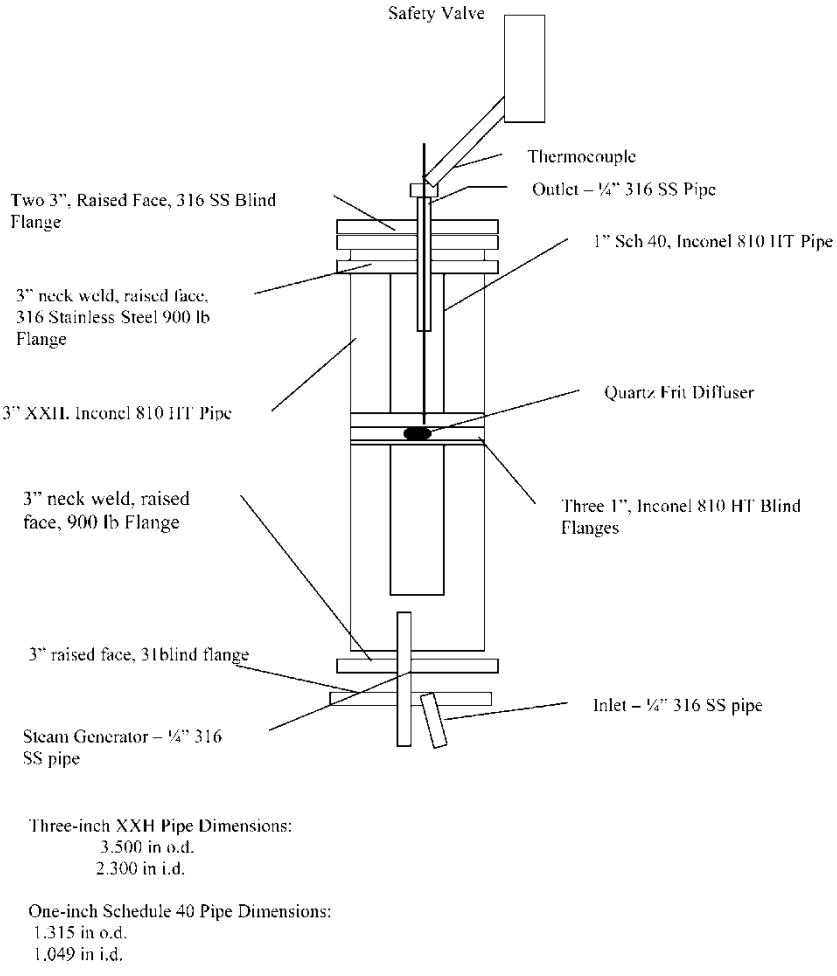

Figure 1. Fluidized bed reactor schematic.

exterior pipe and outlet tube with details shown in Fig. 2. The design allowed for the use of graphite spiral wound gaskets to seal the 900-pound flanges at each end of the reactor, by keeping the flange temperature below 400°C through radiation and convective cooling. The one inch suspended pipe contained a quartz frit welded between two plates to act as a diffuser for the inlet gas. The internal pipe was completely removable, and experienced little differential pressure. The outlet products of the fluidized bed passed through the inner pipe, and to the analysis branch. The seal between the inner and outer pipe was assured by welding the inner pipe to a raised face flange and sealing to the top flange with a graphite gasket. A crane was used to position the reactor for suspension on a steel support.

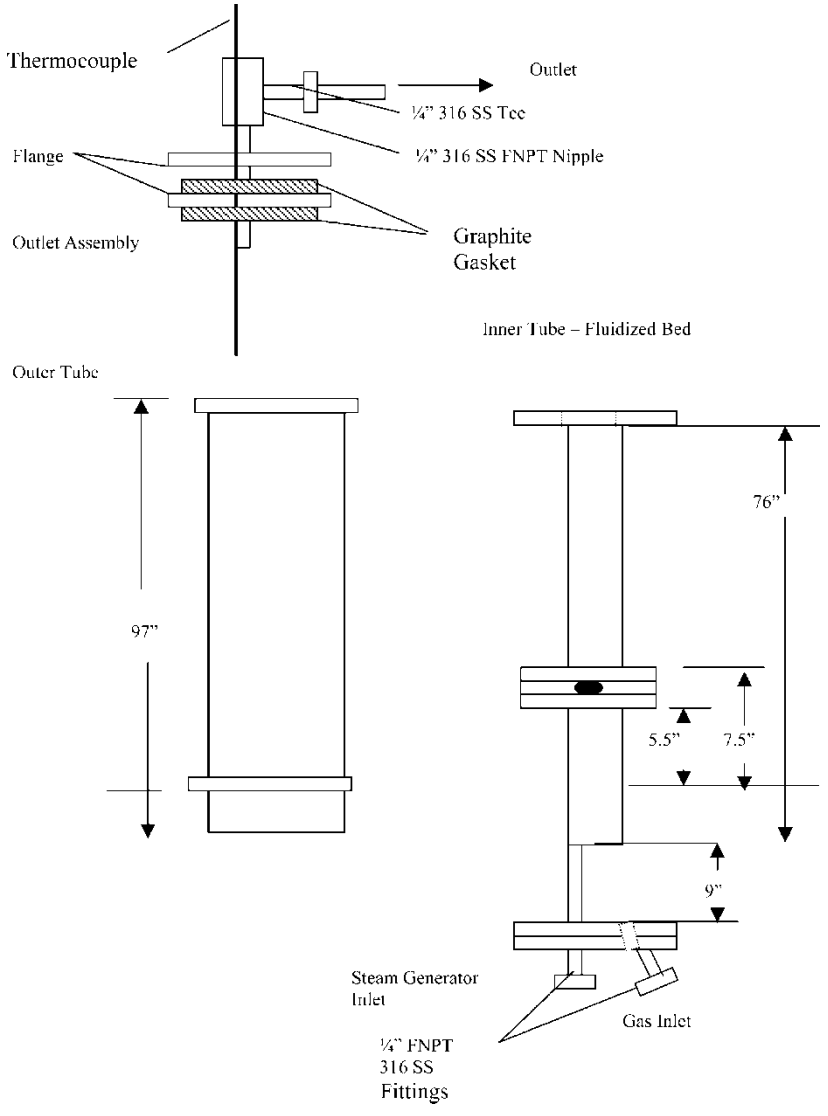

Figure 2. Section details—reactor.

The reactor was heated with a custom high- temperature ceramic furnace and add-on pre-heater. The furnace heated a 41-inch length of the reactor beginning 47 inches below the top flange. This allowed the inlet gas to be heated in a 28-inch length of the reactor before entering the fluidized bed area. The estimated, maximum bed height of 7 inches was designed to be contained within the highest temperature area of the reactor, heated by the custom ceramic furnace. This allowed a 41-inch length of pipe to cool the

gas stream and to provide a disengagement zone by slowing of the exiting gas velocity. Initial testing and observations during experimentation supported the cooling design, with the topmost flanges operating near room temperature at most gas flowrates, and minimum elutriation of solids. Inlet water was preheated to steam through a 6-inch long, $1/4''$ diameter stainless steel pipe constructed within the preheated zone, which allowed the inlet water to reach a temperature above the condensation point before entering the outer tube of the reactor. Water was introduced into the system by a high pressure metering piston pump with minimum flow rate output of 0.1 ml/min, maximum output of 3.0 ml/min and accuracy of $+/-0.3\%$ full scale.

The gas delivery system schematic is shown in Fig. 3 and analysis setup downstream of the reactor is shown in Fig. 4. Gas was provided to the inlet stream through the use of high-pressure tanks. Sierra 820 Series Top-Track Mass Flow Meters and metering valves controlled the inlet flow rate of all inlet gases. Nitrogen was used as a low-pressure purge. The mass flowmeters, when used with a single gas, provided an accuracy of 1.5% of full scale, but when used with the syngas mixture had an accuracy between 5% and 10%. The outlet flowrate was measured with a Sierra 820 Series Mass Flow

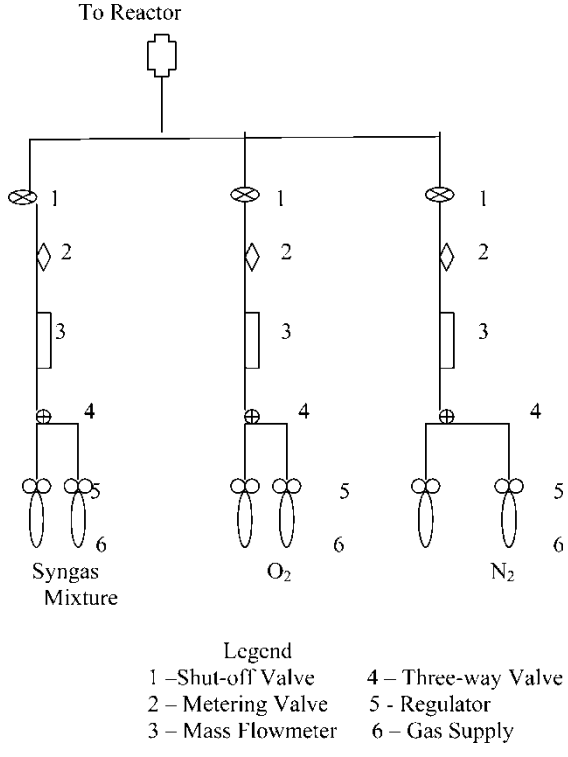

Figure 3. Gas delivery system.

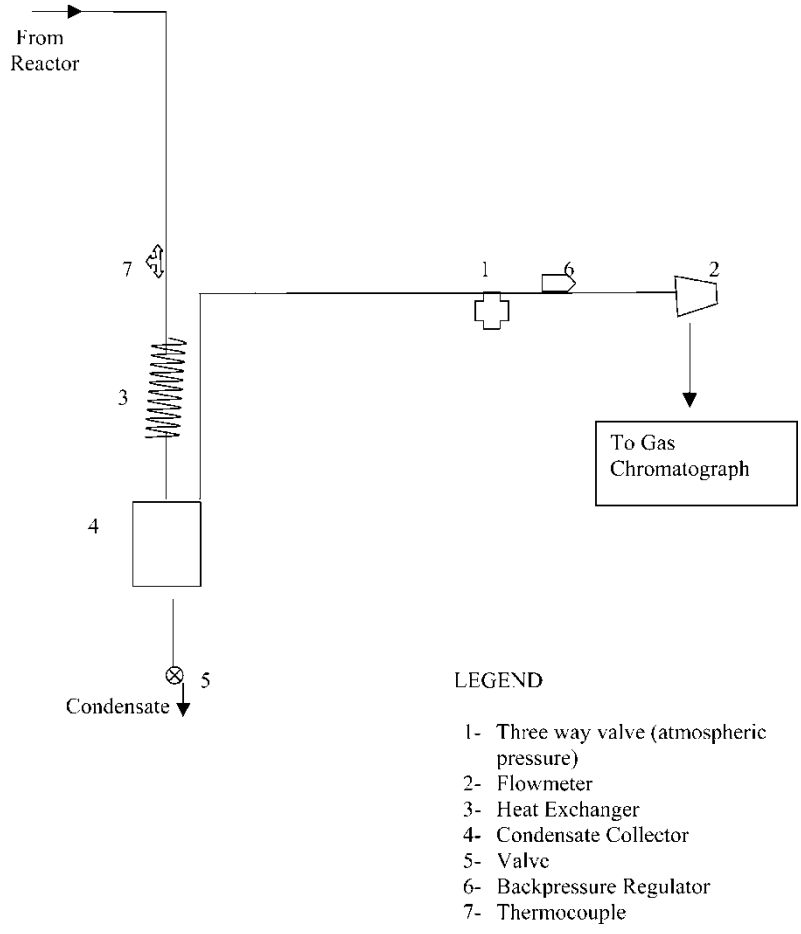

Figure 4. Outlet gas system.

Meter for a portion of the experiments and a Gilmont Accucal variable area flowmeter, with a $+/-10\%$ maximum error (Table 2).

Batch condensate measurement was made with the aid of the cold-water heat exchanger and drain. Outlet gas flow was measured with a variable area flowmeter on some tests and a mass flowmeter on other tests. A Taylor Model 7704 angle body backpressure regulator guaranteed a constant system pressure during the 250 and 515 psi runs. A safety valve was installed parallel to the reactor outlet to protect against runaway pressure increases in the reactor or outlet line.

The outlet below the backpressure valve was open to the atmosphere, to assure a one-atmosphere gas delivery to the gas-monitoring system. A by-pass around the backpressure valve was opened to operate the system at low pressures.

Table 2. Cumulative error in flow rate instrumentation

Accuracy of inlet–syngas mixture	Accuracy of inlet–water	Accuracy of outlet–gas	Maximum cumulative error in flowrate measurement
10%	0.3%	Mass flowmeter – 10% maximum	14.15%
10%	0.3%	Gilmont variable area–10%	14.15%

FLOWRATES

A preliminary cold flow study of the fluidization properties of the iron and calcium compound samples found that the optimum flow rate for a hematite and calcium oxide blend was fifteen times the iron compound minimum fluidization velocity and thirty to forty times the calcium oxide minimum fluidization velocity. Calcium carbonate also exhibited its best fluidization characteristics at thirty times its minimum fluidization velocity. Velocities between minimum and optimum forced the bed to operate under slugging or channeling conditions. Particle diameters of approximately 20 μm were used for the cold flow study.

Using the Ergun equation (Eq. 1) (10)

$$\frac{1.75}{\phi_s \varepsilon_{mf}^3}\mathrm{Re}_p^2 + 150\left(\frac{1-\varepsilon_{mf}}{\phi_s^2 \varepsilon_{mf}^3}\right)\mathrm{Re}_p = \frac{g d_p^3 \rho_g(\rho_p - \rho_g)}{\mu^2} \tag{1}$$

in combination with the effect of temperature and pressure on the physical properties of the fluidizing gas (Eq. 2–10, theoretical linear velocities for 100 μm hematite particles and 20 μm quicklime particles were determined.

Low-pressure viscosity was found using the method of Chung et al. (11)

$$\eta = 40.785\frac{F_c(MT)^{1/2}}{V_C^{2/3}\Omega_V} \tag{2}$$

where

$$\Omega_v = \left[1.16145\left(\frac{kT}{\varepsilon}\right)^{-0.14874}\right] + 0.52487\left[\exp\left(-0.77320\left\{\frac{kT}{\varepsilon}\right\}\right)\right] + 2.16178\left[\exp\left(-2.43787\left\{\frac{kT}{\varepsilon}\right\}\right)\right] \tag{3}$$

and

$$F_C = 1 - 0.2756\omega + 0.059035\mu_r^4 + \kappa \tag{4}$$

Viscosity for gases under high pressures was found using the method of Jossi, Steils and Thodos (11). This method incorporates all temperature effects into a low density viscosity, then compares the residual viscosity between high and low pressure with the fluid density. For nonpolar gases with a reduced gas density range between 0.1 and 3:

$$[(\eta - \eta^0)\xi_T + 1]^{1/4} = 1.0230 + 0.23364\rho_r + 0.58533\rho_r^2 + 0.40758\rho_r^3 - 0.093324\rho_r^4 \tag{5}$$

where

$$\xi_T = \left(\frac{T_C}{M^3 P_C^4}\right)^{1/6} \tag{6}$$

For polar gases:

$$(\eta - \eta_0)\xi_T = 1.656\rho_r^{1.111} \qquad \rho_r \leq 0.1 \tag{7}$$

$$(\eta - \eta_0) = 0.0607(9.045\rho_r + 0.63)^{1.739} \quad 0.1 \leq \rho_r \leq 0.9 \tag{8}$$

$$\log\{4 - \log[(\eta - \eta_0)\xi_T]\} = 0.6439 - 0.1005\rho_r - \Delta \quad 0.9 \leq \rho_r \leq 0.6 \tag{9}$$

where

$$\Delta = (4.75 \times 10^{-4})(\rho_r^3 - 10.65)^2 \quad \text{when } 2.2\langle\rho_r\langle 2.6 \tag{10}$$

and

$$\Delta = 0 \quad \text{when } 0.9 \leq \rho_r \leq 2.2$$

Using the ideal gas law, these values were converted to standard conditions and used as a basis for inlet gas flow.

To make certain the solids were adequately fluidized, the differential pressure across the fluidized bed was monitored by a Capsuhelic Differential Pressure Gauge. The pressure drop across the frit was calibrated with linear fluid velocity. The pressure drop across the frit and solids was then monitored during operation to assure that this drop was equal to the mass of the solids in the bed, a good determiner of fluidization. Some slugging did occur at start-up and channeling was exhibited as the solid agglomerated in the reactor.

RESPONSE SURFACE STUDY

This series of experiments was designed as a statistical analysis to determine an area of optimization for the production of high-purity hydrogen using

pressure and temperature as variable factors. High-purity hydrogen production was defined for this study as a lack of measurable CO_x within the 0.25% error limit of the gas chromatograph used for chemical analysis. The fluidized bed was loaded with 50 grams of the 1 : 7 mass ratio of Fe_2O_3:CaO to assure pressure drops across the bed were within the scale of the differential pressure gauge used to monitor the fluidization quality. Inlet gas was mixed to represent the product of a Vision 21 process and was composed of 44% CO, 33% H_2, and 23% H_2O. This volume percent mixture was introduced by the delivery system at pressures varying between 50 psi and 515 psi and temperatures between 725°C and 800°C. The outlet gases were monitored while the reactor cycled to determine the efficacy of the solids under optimum hydrogen production conditions.

The basic procedure for the production cycle involved:

1. Heating reactor to temperature while fluidizing solids with nitrogen flow to prevent excessive agglomeration
2. Pressurizing reactor with nitrogen
3. Introducing wet syngas for a given period of time
4. Purging with nitrogen at target pressure and temperature
5. Depressurizing slowly to prevent elutriation of solids
6. Cool-down with no gas flow

Outlet gas was collected every minute during active reaction times and every five minutes or longer during purging. The samples were analyzed using a Gas Chromatograph Series 600, GOW-MAC Instrument Company with a Restek Rt-QPLOT Column, sensitive to CO_2. Water was condensed from the outlet stream and measured as a batch quantity. Solids were removed after cool down, weighed and photographed. Select samples were analyzed through x-ray diffraction. Other parameters measured included inlet and outlet flow rate, temperature, and pressure.

Chemical properties and sources of the solids used in the experiments are listed in Tables 3 and 4. Contaminants in the calcium oxide were limited to 2% by weight and did include CO_2, $CaSO_4$, Fe_2O_3, and Al_2O_3. The Fe_2O_3 sample contained 99.6% hematite by weight. A small amount of FeO was present with 0.1% other contaminants. Weighted average diameters of the hematite and quicklime were determined by a Micro-Trac Particle Analyzer and found to be 100 μm and 20 μm, respectively. Flow rate of the syngas into the bed was consistent with 15 times minimum fluidization for the 100 micrometer average diameter of the ferric oxide and 30–40 times minimum fluidization velocity for the 20 micrometer average diameter of the CaO particles, as determined in the fluidization study.

A factor-response table for the study design is shown in Table 5 and was used as the foundation for a response surface analysis of optimum conditions for high purity hydrogen in the outlet stream.

Table 3. Typical chemical analysis by weight of calcium oxide sample vertical pulverized quicklime Mississippi Lime Company Alton, IL

Element	Percent
CaO Total	98.0
CaO Available	95.0
CO_2	0.40
Acid Insolubles	0.20
$CaSO_4$	0.04
S – Equivalent	0.01
SiO_2	0.75
Al_2O_3	0.10
Fe_2O_3	0.05
MgO	0.50
LOI	0.50
P_2O_5	0.010
MnO	0.0015

Table 4. Chemical properties of Fe_2O_3 sample (percent by weight dry basis) H-25 Iron oxide powder CAL Fe_2O_3 Pea Ridge Iron Ore Company Sullivan, MO

Element	Percent
Fe_2O_3	99.6
FeO	0.3
SiO_2	0.21
CaO	0.04
Al_2O_3	0.02
MgO	0.03
Na_2O	0.005
K_2O	0.002
P	0.015
Mo	<0.001
Cu	<0.002
Ni	0.012
F	<0.01
Cl	<0.01
MnO	0.035
S	0.005
TiO_2	0.065
Cr	0.006
H_2O	0.03

Both temperature and pressure, either alone or interacting with each other, were significant in the production of all outlet gases within a 95% probability, as shown in Table 6. The conditions producing the least CO/CO_2 and greatest percentage of H_2 in the outlet were at the lowest pressures and temperatures. This is illustrated by the response surface plots, produced by Design-Expert Software, a product of DesignEase and shown in Figs. 5 through 8. However, the most significant factor effecting the production of mass of hydrogen was pressure, with the greatest mass produced by the highest pressures, presumably because of the higher standard flow rates.

One surprising result of the analysis of the outlet gas was the discovery of methane. In the shake down experiments, a significant amount was produced. This was apparently the result of the methanation of COx catalyzed by the high nickel content of the Inconel reactor walls. The linear relationship between pressure and CH_4 production shown in Fig. 7 supports this theory. Increasing pressure would increase the diffusion of the gases into the walls of the reactor where it can be catalyzed by the nickel in the alloy.

Carbon was also deposited on the walls of the reactor most likely due to the Bouduard Reaction. It is well known that Bouduard progresses toward the forward reaction near 873 K with small CO concentrations. Although the fluidized bed portion of the reactor was always set at 998 K or above, the reactor was designed with a significant thermal gradient to allow the use of manufactured graphite gaskets. It was noted that carbon deposition occurred in the outer shell area and in the inlet of the inner Inconel tube. This also coincided with areas of temperature less than 900 K. No carbon deposition was ever noted at the outlet, probably due to the low carbon dioxide concentrations.

In order to suppress methane production due to the effects of the reactor walls, a paintable ceramic liner was applied to the outer shell and inlet area of

Table 5. Factor-response for initial response surface study of hydrogen production

		Response				
Factor Temperature (C)	Pressure (psi)	Maximum % H_2 (15 min)	Maximum % CO (15 min)	Maximum % CO_2 (15 min)	Maximum % CH_4 (15 min)	Mass of pure H_2 (g)
750	50	97.8	0	0	5.4	0.07054
800	515	94.2	15.2	8.4	18.4	1.26625
725	50	98.8	0	0	3.9	0.08945
725	515	60.7	24.7	29.5	35.4	0.67148
750	250	92.3	0	0	22.0	0.41246
725	250	96.8	0	0	19.9	0.38532
800	50	81.7	20.6	20.5	4.1	0.073328
800	250	95.5	7.9	2.8	7.2	0.59903

Table 6. Significant effects on production response

Response	Significant factors (95%)	F-value	P-value	Surface model	R^2 (FIT)
Percentage of H_2	Temperature-pressure interaction	43.19	0.0224	Quadratic	0.9729
Percentage of CO	Temperature-pressure interaction	28.83	0.0330	Quadratic	0.9762
Percentage of CO_2	Temperature	31.18	0.0314	Quadratic	0.9873
	and temperature-pressure interaction	78.99	0.0124		
Percentage of CH_4	Temperature	6.99	0.0458	Linear	0.8677
	pressure	27.06	0.0035		
Mass of H_2 in 15 minutes	Temperature	217.91	0.0001	2FI	0.9981
	pressure	1709.91	<0.0001		
	Temperature-pressure interaction	169.99	0.0002		

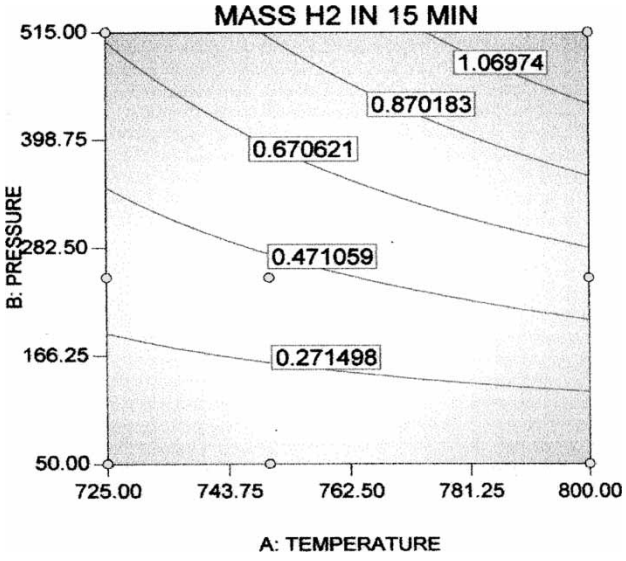

Figure 5. Response surface results of mass of high-purity hydrogen produced in 15 minutes.

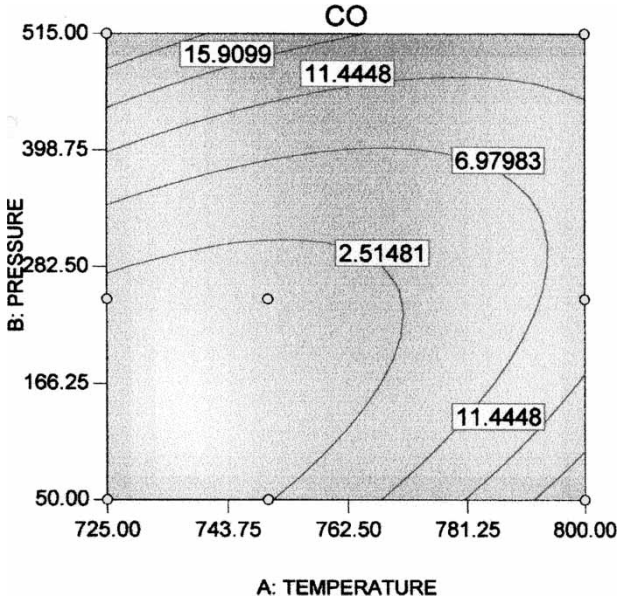

Figure 6. Response surface results of percentage of CO appearing in outlet gas in first fifteen minutes.

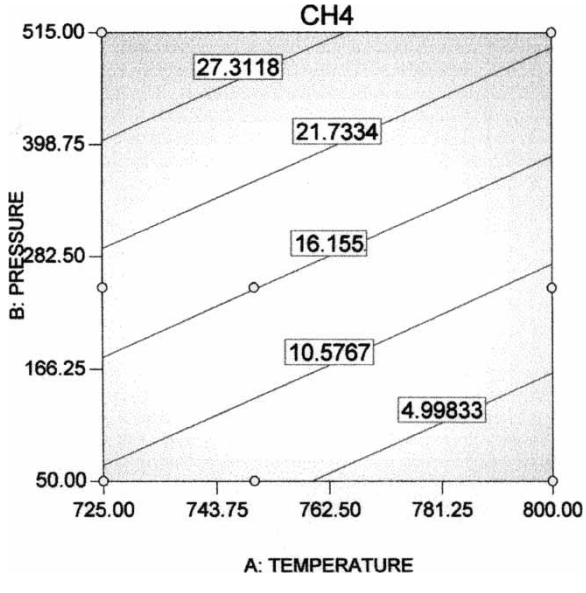

Figure 7. Response surface results of percentage of CH_4 appearing in outlet gas in girst fifteen minutes.

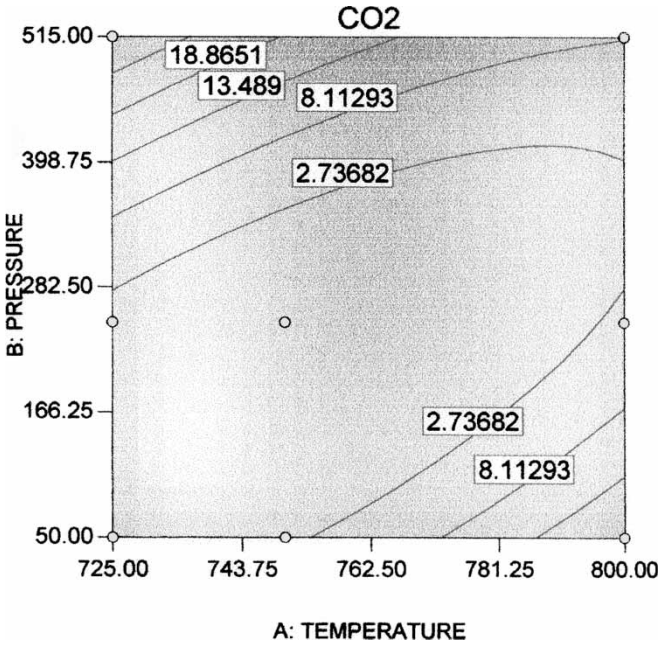

Figure 8. Response surface results of percentage of CO_2 appearing in outlet gas in first fifteen minutes.

the inner shell. This dramatically decreased methane production, but did not stop it completely, especially at high pressures. This coincides with the statistical analysis of a linear relationship between the effects of temperature and pressure with the production of methane. Small cracks and blemishes developed in the liner, which exposed portions of the reactor walls to CO_x gases. An increase in pressure produced a greater concentration gradient within the walls, which acted as a catalyst for the methane production.

The model of CO/CO_2 production versus pressure and temperature are shown in Figs. 6 and 8. In general, an increase in temperature at a constant pressure is predicted to increase the percentage of CO_x in the outlet gas, confirming the increase of the chemical reaction rate of CO_x production with temperature. The significance of chemical reaction compared to diffusion is further illustrated by the fact that the model predicts similar CO and CO_2 outlet concentrations at the same temperature, but different pressures. This is especially notable at lower pressures.

While the methane production increased linearly with pressure between 725°C and 800°C, with maximum development at higher pressures, the mass of CO_x in the output gas composition was zero for the minimum fifteen minute testing period at all combinations of 725°C, 750°C and 50 psi, 250 psi. Although high-purity hydrogen (no CO_x) was also produced

at these combinations, the greater mass of hydrogen in the output occurred at higher pressures because of the higher flow rates required for fluidization under these conditions. This is confirmed by the statistical finding that the mass of high-purity hydrogen produced during the fifteen minute testing interval increased most significantly with pressure.

In combining the results, the maximum high-purity hydrogen production occurred in the vicinity of 725°C and 250 psi.

X-RAY DIFFRACTION ANALYSIS OF SOLIDS AFTER PRODUCTION

The lack of $Fe_2O_3$and Fe_3O_4 in the x-ray diffraction results indicated that the length of each run was appropriate to reduce the iron without allowing re-oxidation, with the exception of the 725°C, 250 psi experiment. Input of reactant gases for conditions of 800°C, 250 psi; 725°C, 50 psi; and 725°C, 250 psi was extended in order to determine the limits for high-purity hydrogen production and to catch the limit of CO_x adsorption. The 40 minutes used for input of syngas was too long, and allowed the re-oxidation of the FeO.

Iron Carbide was found under all conditions except 725°C, 250 psi and 725°C, 50 psi. The carbonation of iron only occurs near the completion of the decomposition process and the formation of elemental iron. Adjusting the inlet gas composition and/or shortening production time should prevent FeC formation by limiting the extent of the decomposition of the iron compounds.

At 725°C and 50 psi, only $CaCO_3$ and $Ca(OH)_2$ are present, with no CaO indicated. However, both CaO and $CaCO_3$ are present in the results for all combinations of temperatures at 250 psi and at 725°C and 515 psi. Since higher partial pressure of CO_2 should shift the calcium reaction toward carbonation, the appearance of CaO is probably a result of the observed agglomeration and possible surface changes in the pore structure. The inability of the CaO to adsorb all CO_2 in the reaction at 800°C and 250 psi is most likely a result of a combination of agglomeration/surface pore clogging and the decomposition shift caused by higher temperature.

CONCLUSIONS

The initial response surface experiments were designed to determine the optimum conditions for the production of high-purity hydrogen from wet syngas using 50 grams of a 1 : 7 mass ratio of Fe_2O_3:CaO loaded into the fluidized bed reactor. Pressure was varied between 50 psi and 515 psi and temperature between 725°C and 800°C in a response surface study. Results indicated:

- Optimum hydrogen production (largest mass in 15 minutes with no CO_x) occurred near conditions of 725°C and 250 psi.

- Mass of produced high-purity hydrogen increased most significantly with pressure.
- CO_x production was zero for 15 minutes of monitored output at combinations of 725°C and 50 psi, 250 psi.
- Methane production increased linearly with pressure due to the catalytic effect of the high nickel content of the reactor walls.
- The chemical reaction is predicted to be a controlling factor in the percentage of CO and CO_2 in the outlet at lower pressures.

DEFINITION OF VARIABLES

k	Boltzmann's Constant
K	association factor
M	molecular weight
P	Pressure
P_c	critical pressure
P_r	Reduced gas pressure = P/P_c
T	temperature
T_c	critical temperature
T_r	reduced gas temperature = T/T_c
V_c	critical volume
ρ_r	reduced gas density = $\rho/\rho_c = V_c/V$
η	dense gas viscosity ((μP)
Ω_v	viscosity collision integral
ξ_T	$(T_c/M^3P_c^4)^{1/6}$ in μP^{-1}
ω	acentric factor = $-\log P_r$ (at $T_r = 0.7$) − 1.000
κ	correction factor for highly polar substances
ε_{mf}	bed void fraction at minimum fluidization
ε	void fraction
d_p	particle diameter
g	acceleration of gravity
Re_p	particle Reynold's number
ρ_c	critical density
ρ_g	gas density
ρ_p	solid density
μ	dynamic gas viscosity
ϕ_s	sphericity = area of particle/area of sphere of same radius
η_o	low pressure gas viscosity (μP)

ACKNOWLEDGEMENT

The authors are pleased to acknowledge the U.S. Department of Energy (contracts DE-FC26-00FT40974 and DE-FC26-03NT41842) and General Electric for their financial support.

REFERENCES

1. Han, C. and Harrison, D. (1994) Simultaneous Shift Reaction and Carbon Dioxide Separation for the Direct Production of Hydrogen. *Chemical Engineering Science*, 49: 5875.
2. Perry, J., Chilton, C., and Kirkpatrick, S. (1963) *Chemical Engineers' Handbook*; 4th Ed., McGraw-Hill: New York.
3. Turkdogan, E.T. and Vitners, J.V. (1971) Gaseous Reduction of Iron Oxides: Part I. Reduction of Hematite in Hydrogen. *Metallurgical Transactions*, 2: 3175.
4. Turkdogan, E.T. and Vitners, J.V. (1971) Gaseous Reduction of Iron Oxides: Part III. Reduction-Oxide of Porous and Dense Iron. *Metallurgical Transactions*, 3: 1561.
5. Szekely, J. and El-Tawil, Y. (1972) The Reduction of Hematite Pellets with Carbon Monoxide-Hydrogen Mixtures. *Metallurgical Transactions*, 2: 3175.
6. Doherty, R.D., Hutching, K.M., Smith, J.D., and Yoruk, S. (1985) The Reduction of Hematite to Wustite in a Laboratory Fluidized Bed. *Metallurgical Transactions B*, 33: 425.
7. Boynton, R. (1966) *Chemistry and Technology of Lime and Limestone*; John Wiley & Sons: New York, N.Y.
8. Borgwardt, R.H. (1984) Calcium Oxide Sintering in Atmospheres Containing Water and Carbon Dioxide. *Ind. Eng. Chem. Res.*, 28: 493.
9. Han, C. and Harrison, D. (1997) Multicycle Performance of a Single-Step Process for H_2 Production. *Separation Science and Technology*, 32: 681.
10. Kunii, D. and Levenspiel, O. (1969) *Fluidization Engineering*; John Wiley & Sons, Inc.: New York, N.Y.
11. Reid, R., Prausnitz, J., and Poling, B. (1987) *The Properties of Gases and Liquids*; 4th Ed., McGraw-Hill Book Co.: New York, N.Y.